

Nanogrooved Elastomeric Diaphragm Arrays for Assessment of Cardiomyocytes under Synergistic Effects of Circular Mechanical Stimuli and Electrical Conductivity to Enhance Intercellular Communication

Abdullah-Bin Siddique, Keith A. Williams, and Nathan S. Swami*



Cite This: *ACS Biomater. Sci. Eng.* 2025, 11, 672–681



Read Online

ACCESS |



Metrics & More



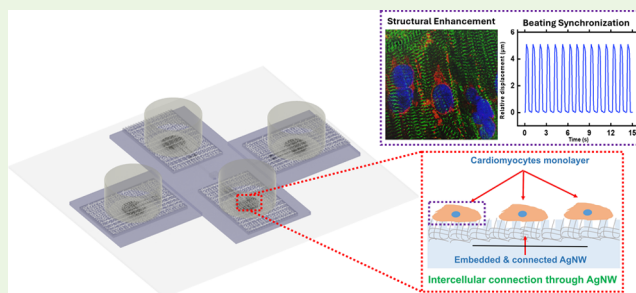
Article Recommendations



Supporting Information

ABSTRACT: Cardiovascular diseases remain the leading cause of mortality, necessitating advancements in *in vitro* cardiac tissue engineering platforms for improved disease modeling, drug screening, and regenerative therapies. The chief challenge to recapitulating the beating behavior of cardiomyocytes is creation of the circular stress profile experienced by hollow organs in the natural heart due to filling pressure and integrated strategies for intercellular communication to promote cell-to-cell connections. We present a platform featuring addressable arrays of nanogrooved polydimethylsiloxane (PDMS) diaphragms for cell alignment and circular mechanical stimulation, with embedded silver nanowires (AgNWs) for electrical cues, so that cardiomyocyte functionality can be assessed under these synergistic influences. Central to our innovation is a two-layer PDMS diaphragm design that electrically isolates the liquid metal (EGaIn) strain sensor in the bottom layer to enable detection and control of mechanical stimulation from conductive portions of embedded AgNWs in the top layer that supports cardiomyocyte culture and communication. In this manner, through localized detection and control of the circular mechanical stimulation, the essential role of multiaxial stretching on cardiomyocyte function is elucidated based on their contractility, sarcomere length, and connexin-43 expression. This *in vitro* platform can potentially transform cardiac tissue engineering, drug screening, and precision medicine approaches.

KEYWORDS: cardiomyocyte cell maturation, beating synchronization, PDMS diaphragms, nanogrooves, Ag nanowires



The high mortality rates of cardiovascular diseases worldwide have motivated advancements in cardiac tissue engineering for improved disease modeling, drug screening, and regenerative medicine.¹ A key challenge in this field is the development of *in vitro* biomimetic platforms that replicate the physiological environment of the heart² to recapitulate the beating behavior of cardiomyocytes using actuators for mechanical stimulation. Due to the tunable mechanical properties of polydimethylsiloxane (PDMS),^{3–7} microfabricated PDMS diaphragms have emerged as promising substrates for cardiomyocyte culture and stimulation.^{8,9} Several recent works have combined soft lithography and microfluidics for the design and fabrication of PDMS-based cardiomyocyte platforms through the creation of microscale features on PDMS substrates, such as grooves, channels, and pillars, which play a crucial role in directing cardiomyocyte alignment, maturation, and electrophysiological properties.^{10–13} Subsequently, the integration of electrical and mechanical stimulation components into PDMS matrices has facilitated the development of sophisticated cardiac models capable of mimicking the dynamic nature of the cardiac

microenvironment for measurement of cardiomyocyte response to physiological cues and external stimuli.^{14,15}

PDMS-based platforms offer unprecedented opportunities for *in vitro* studies on cardiomyocyte physiology,¹⁶ drug responses,¹⁷ and disease mechanisms.¹⁸ These platforms seek to recapitulate cardiac function, including contractility, electrophysiology, and tissue architecture, to provide insights into cardiac development, pathology, and therapeutic interventions, using external mechanical and electrical cues.^{19–24} Pavesi et al. explored a microscale cell stimulator capable of simultaneous mechanical, electrical, and biochemical stimulation on stem cells that enabled rapid sample processing and precise fluidic control, thereby allowing for detailed analysis of cellular responses, including morphological changes and gene

Received: July 14, 2024

Revised: November 5, 2024

Accepted: December 3, 2024

Published: December 16, 2024



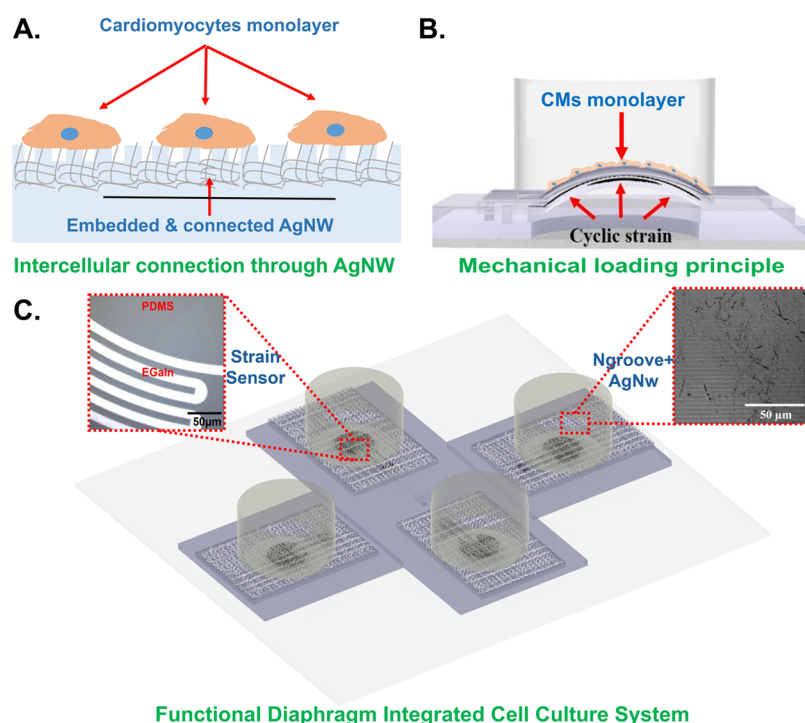


Figure 1. (A) Cross sectional view of cultured cardiomyocyte monolayer on AgNW-embedded PDMS diaphragm. (B) Representation of mechanical stimulation technique of cardiomyocytes using this platform. (C) Schematic illustration of the array platform for promoting cardiomyocytes growth and intercellular communication (inset on the left shows the integrated liquid metal sensor and on the right shows embedded Ag-NWs within the nanogrooved PDMS).

expression.²⁵ Nitsan and colleagues utilized a mechanical probe on a pliable cardiomyocyte culture surface to prompt their synchronized beating at the stimulation frequency.²⁶ Meanwhile, Sidorov and team introduced a uniaxial stretcher designed to longitudinally align cultured cardiomyocytes, thereby enhancing their contractile strength.²⁷ However, these platforms do not accurately simulate the circular stress profile experienced by hollow organs in the natural heart due to filling pressure,^{28,29} leading to the limited influence on cell response by mechanical cues and intercellular communication strategies to improve cell-to-cell connections. Additionally, cardiomyocytes cultured on these platforms showed a random distribution and multipolar morphology, unlike the rod-shaped and oriented cardiomyocytes found *in vivo*.^{30,31} Overcoming this challenge requires innovative micro/nanofabrication approaches that support cellular viability and intercellular interactions with integrated structures that can detect and control mechanical stimuli.

Nanostructured grooves on soft materials have emerged as a promising platform to direct cell alignment³² and promote intercellular communication under mechanical loading conditions. The circular geometry of PDMS diaphragms offers distinct advantages, in terms of uniform stress distribution and scalability, which are crucial for achieving reproducible cellular responses across the engineered tissue.^{9,29,33} Additionally, the incorporation of conductive materials, such as gold and Ag nanowires (AgNWs) into PDMS, enables conductive substrates that can enhance the electrical communication of cardiomyocytes. In this context, Kim et al. proposed a microgrooved (rather than nanogrooved) PDMS membrane with AgNWs to improve maturation and drug-induced cardiotoxicity evaluation, with the cultured cardiomyocytes showing significant improvements in contraction force,

sarcomere length, and Cx43 expression.³⁴ Jeong et al. used a circular diaphragm with a conductive thin gold layer and nanogroove patterns to mechanically stimulate cardiomyocytes at 6% strain, observing enhanced sarcomere orientation and increased Cx43 expression.³⁵ Dou and colleagues explored multiaxial stresses on cytoskeletal organization and structural development of cardiomyocytes under varying mechanical stimulations.³³

The integration of nanogrooves for cell alignment along with stimulated elastomeric diaphragms to create a circular stress profile on cardiomyocytes that are cultured on a conductive AgNW-embedded surface would allow for direct optimization of the synergistic effects of cell alignment, mechanical stimulation, and improved intercellular communication. However, integration of these components is limited by the biocompatibility of AgNWs on the nanogrooved substrate and electrical interference of the AgNWs with the embedded strain sensor that is needed to measure and control the mechanical stimulation level. To overcome this, we implement a two-layer diaphragm design that electrically isolates the liquid metal strain sensor in the bottom layer from conductive portions of the top layer, which is optimized for the proportion of embedded AgNWs to support cardiomyocyte culture. Based on this innovation, we present a nanogrooved array platform for biomimetic cell culture, featuring four individual wells for culture and assessment cardiomyocyte morphology and function. Each well incorporates a nanogrooved circular PDMS diaphragm embedded with AgNWs to create cell alignment, integrated with a liquid metal (EGaIn) strain sensor to quantify the effect of mechanical stimulation on cardiomyocyte function. The synergistic effects of mechanical stimulation and improved intercellular communication on cultured cardiomyocytes are correlated with their beat rate

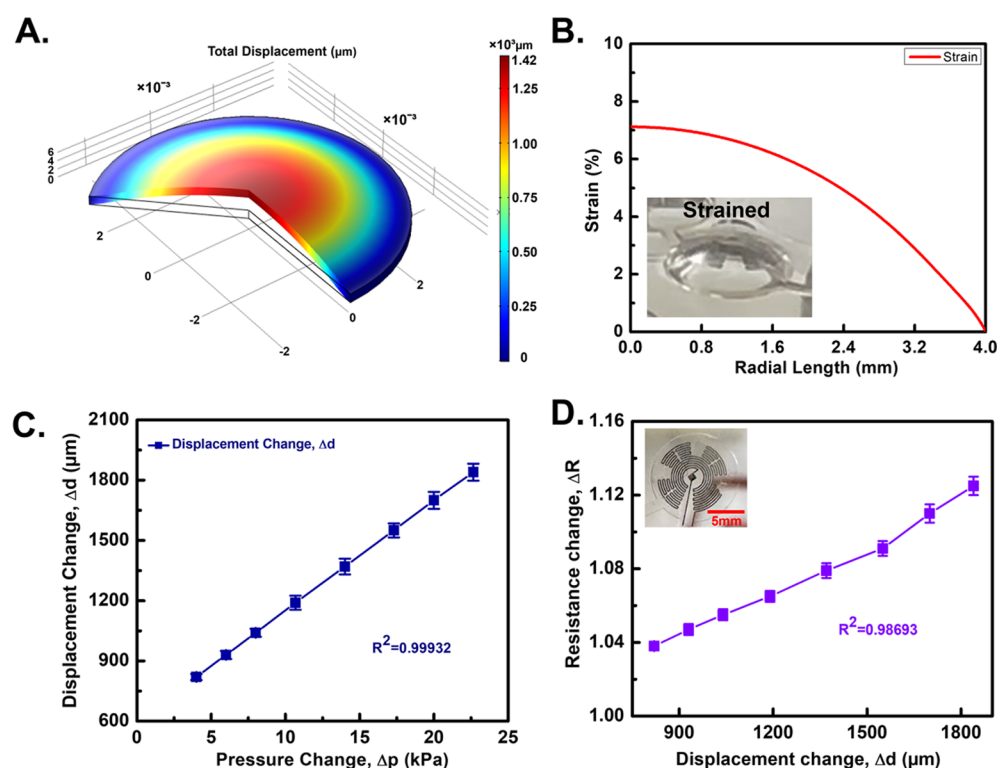


Figure 2. (A) Volumetric displacement profile of the functional PDMS diaphragm. (B) Strain profile of the functional PDMS diaphragm under 7% mechanical loading. (C) Relationship between the change in applied pressure and PDMS diaphragm displacement under different loading conditions. (D) Change in resistance for the integrated EGAIn-based strain sensor at different applied displacement (inset shows EGAIn integrated circular PDMS diaphragm).

through motion tracking and contractility based on alterations in sarcomere length and connexin-43 expression after immunofluorescence staining analysis.³⁶ Such nanogroove array platforms for cardiomyocyte culture and functional evaluation under synergistic stimulation are essential for translation toward drug screening and precision medicine applications using patient-derived materials.^{37–39}

RESULTS AND DISCUSSION

Device Principle. Figure 1 illustrates the architecture of the nanogrooved array platform for biomimetic cell culture under external mechanical stimuli (fabrication details in Supporting Information, Figure S1). It features four distinct cell culture wells, each equipped with a functional two-layer PDMS diaphragm. Starting with 800 nm grooves on PDMS to promote cell alignment, AgNWs are embedded in the top layer to create a conductive surface to enhance intercellular communication, while the bottom layer includes a channel to be filled with EGAIn to function as a strain sensor to measure and control the applied force on the cultured cardiomyocytes, periodically applied through the included air inlet (Figure 1A). Using imaging and elemental analysis (Supporting Information, Figures S2 and S3) to visualize the distribution of AgNWs and cell morphology, the AgNW level is optimized for surface conductivity levels of ~ 1.5 M Ω due to embedded AgNW networks, which is close to the resistance levels of 2–400 M Ω reported for native cardiac tissues.⁴⁰ The cyclic pressure applied through the air inlet to embedded microchannels into the supporting PDMS layer causes the addressed diaphragm in each well to bulge, thereby mechanically stimulating the cardiomyocytes (Figure 1B). The enlarged view (Figure 1C)

shows the array with four separate wells along with optical images of the integrated EGAIn-based strain sensor and embedded AgNWs in the nanogrooved platform. The repeatability of the arrayed platform for multiplexed stimulation and cell maturation is presented in Supporting Information, Figure S4. The real-time measurements of resistance from all four wells (Figure S4A) highlight the negligible variations among the resistors and the ability to rapidly detect strain under mechanical stimulation. Figure S4B features images of cultured cardiomyocytes in the four wells, wherein cells are seen to grow uniformly along the nanogrooves. To ensure even translation of the stimulation across all wells, the beating behavior of cells from all four wells was assessed based on real-time videos. Analysis using motion tracking software reveals synchronous cell beating in response to applied mechanical stimulation in all wells (Supporting Information, Movie M1), with negligible differences (Supporting Information, Figure S4C).

Strain Sensor Characterization. Characterization of the integrated EGAIn-based strain sensor is shown to validate its quality, accuracy, and reliability under mechanical loading to ensure consistent and precise measurements. Figure 2 illustrates the initial characteristics of the EGAIn strain sensor integrated with the AgNW-embedded nanogroove PDMS diaphragm. Herein, the relationship between pressure variations induced by the pump and the corresponding displacement of the PDMS diaphragm is examined, with the displacement measured using confocal microscopy. The measured displacement is correlated with strain alterations using finite element analysis simulations in the 2D axis symmetry mode to provide estimates of measured strain based on the PDMS properties (800 kPa Young's modulus, 0.95 kg/

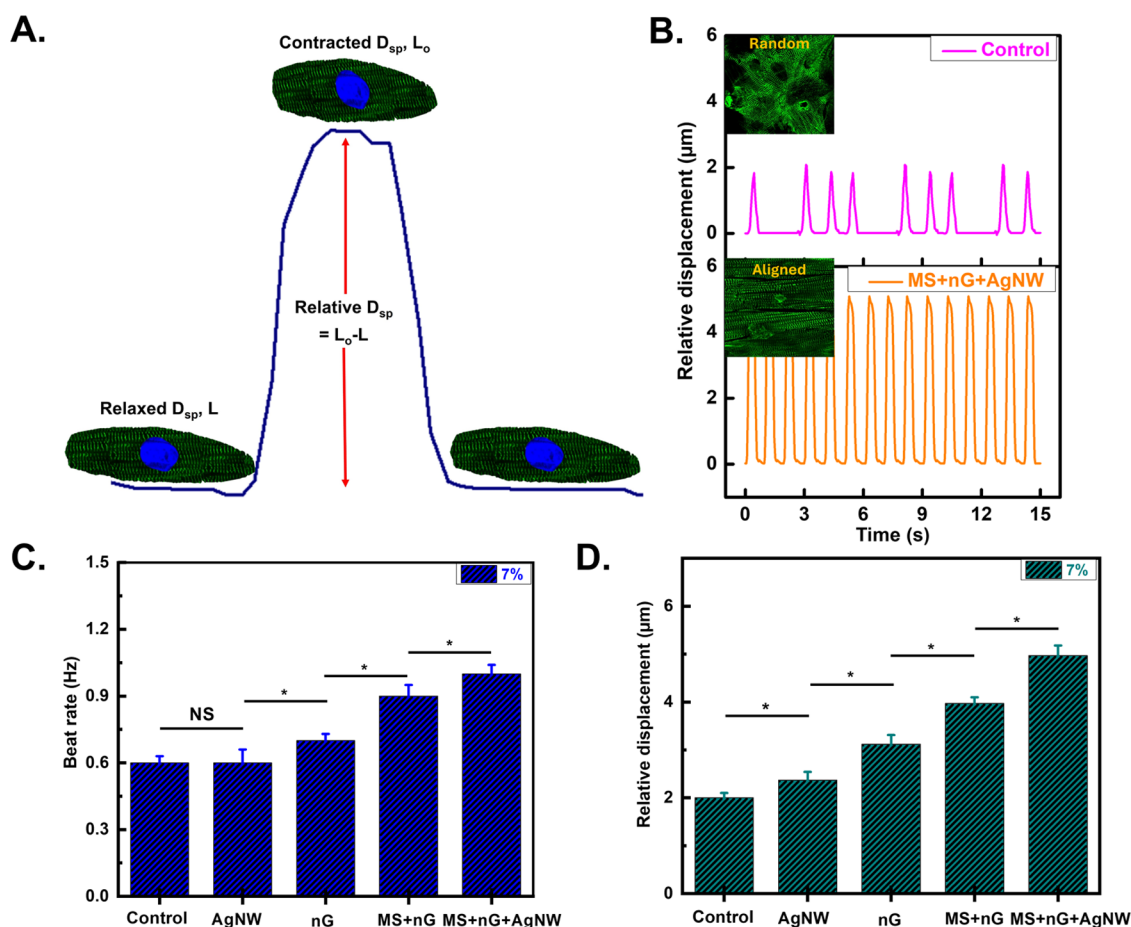


Figure 3. (A) Detection principle of contractile behavior of cardiomyocytes by measuring (cellular displacement or D_{sp} and cellular length or L as indicated). (B) Real time cell beating behavior of cardiomyocytes, cultured on flat PDMS circular diaphragm (control) vs on functional PDMS diaphragm containing nanogrooves and Ag-NWs, (respective stained photographs of cardiomyocytes shown in the inset). (C) Beat rate of cardiomyocytes cultured on different substrates: flat PDMS circular diaphragm (control), an AgNW-embedded circular PDMS diaphragm (AgNW), a nanogrooved circular PDMS diaphragm (nG), a nanogrooved circular PDMS diaphragm under mechanical stimulation (MS + nG), and the AgNW-embedded nanogrooved circular PDMS diaphragm under mechanical stimulation (MS + nG + AgNW). (mechanical stimulation was provided at a strain level of 7% at 1 Hz). (D) Contractility of cardiomyocytes of the respective surfaces from (C) (mechanical stimulation at 1 Hz).

m^3 density, and a Poisson's ratio of 0.49). While strain levels of 12% could be obtained within the applied pressure range for the $\sim 300 \mu m$ thick diaphragms of the current work, we chose 7% loading since it was high enough to fall within the 5–10% strain levels required to improve functional maturation of cultured cardiomyocytes,³⁵ while avoiding pathological responses at higher strains.³³

Representative volumetric displacements of the circular AgNW-embedded nanogrooved PDMS diaphragm under 7% mechanical loading are shown in Figure 2A. The strain profile of the circular PDMS diaphragm under these loading conditions as a function of radial distance from the diaphragm center is shown in Figure 2B. While the strain is highest at the center (7%), it drops off at the diaphragm edge. We chose the central 2 mm region of the diaphragm for cardiomyocyte culture since its strain profile exhibits minimal change. Based on this strain profile, strain sensors were placed at the center of each diaphragm to achieve maximum strain and ensure highly sensitive resistance changes. A positive pressure was applied to bulge the flexible diaphragm (inset of Figure 2B) so that the mostly linear relationship between pressure (4 to 23 kPa) and diaphragm displacement can be used to compute the exact

strain value (Figure 2C). At a pressure of approximately 16.5 kPa, the diaphragm shows a deformation of $\sim 1400 \mu m$, which is equivalent to 7% strain. The resistance values at these displacements were then measured to establish the relationship between displacement change and resistance change since the sensors are to be used to monitor and control mechanical stimulation (Figure 2D). The initial sensor resistance was $\sim 79.2 \Omega$, closely aligning with the theoretical value of 80Ω . Resistance changes were measured by dividing the altered resistance value by the initial resistance value to mitigate fabrication inconsistencies. The sensors demonstrated linear behavior versus diaphragm deformation, highlighting their utility for the real-time monitoring of applied stimulation. The EGaIn-based sensors were used for monitoring mechanical stimulation of cardiomyocytes cultured over 5 days. The long-term durability of the strain sensor is crucial for determining the efficacy of the biosensing platform. Therefore, stability of the sensor toward measuring changes in applied mechanical stimulation is vital for achieving the desired stimulation levels. The sensor stability was assessed daily over a month based on average resistance change, which shows negligible changes from day 0 to day 30 (Figure S5). Under 7% mechanical

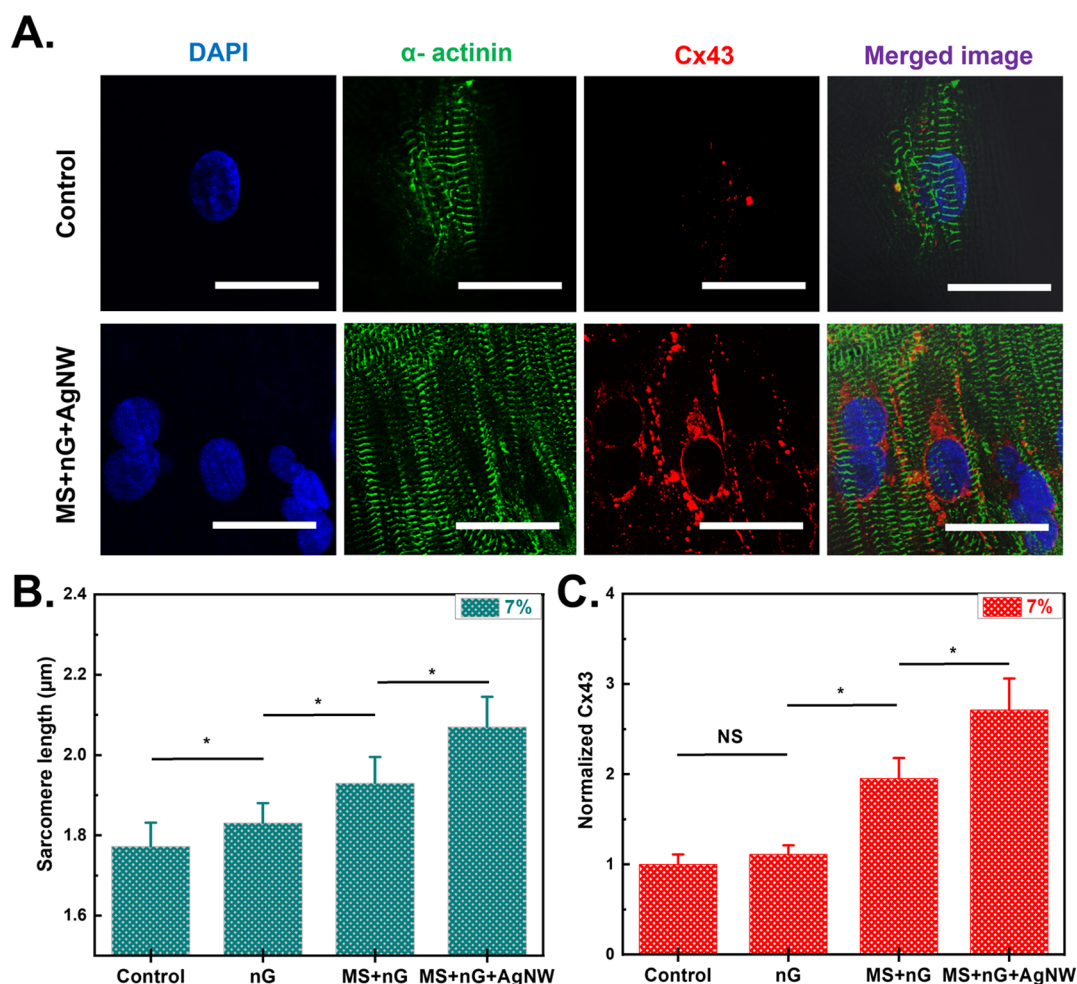


Figure 4. (A) Immunocytochemistry (ICC) stained imaging illustrates the effect of the circular PDMS diaphragms conditions on the cardiomyocyte culture on flat (control), nanogrooved (nG), mechanically stimulated nanogroove (MS + nG), and mechanically stimulated AgNW-embedded nanogrooved substrates (MS + nG + AgNW) (blue, green, and red indicate DAPI, α -actinin and connexin 43 respectively) (scale bar indicates 50 μ m). (B) Quantitative analysis of change in the sarcomere length of cardiomyocytes growing on different culture substrates and conditions. (C) Quantitative analysis of change in connexin 43 expressions of cardiomyocytes growing on different culture substrates and conditions.

stimulation, the long-term study shows an error margin of <2%, with no evidence of fatigue or hysteresis during these prolonged measurements. The long-term stability test, wherein strain sensors were subjected to constant mechanical loading, showed excellent repeatability and stability, indicating the high reliability of the integrated strain sensors.

Cardiac Contractility Quantification. Quantifying cardiac contractility within *in vitro* platforms is essential for assessing cardiac cell and tissue function, as well as for understanding disease mechanisms to enable high-throughput screening of pharmacological effects, cardiotoxicity, and to explore genetic impacts on cardiac function for personalized medicine.^{37–39} In this work, the contractile behavior of cardiomyocytes is analyzed through custom software to observe utilization of the reported platform for cardiomyocyte maturation. Using an inverted microscope, live images and videos of cultivated cardiomyocytes were captured. Motion tracking software was then used to evaluate the contractility of these cells from the recorded videos. The software analyzed the beating activity of each cardiomyocyte over time. To improve the reproducibility of the contractility measurements, at least 10 cells were tracked within each well. The translation of

cardiomyocytes during contraction and relaxation was measured as the relative displacement of cardiomyocytes (Figure 3A). Impact of the synergistic combination of AgNWs, nanogrooves, and circular mechanical stimulation on cardiac contractility was evaluated by comparison with the respective properties of cultured cardiomyocytes grown on flat PDMS diaphragms. Mechanical stretching promotes cellular organization and improves cardiac functions *in vitro* by recapitulating the *in vivo* heart pumping operation. However, the magnitude of the applied external mechanical stretch should be chosen to provide sufficient stimulation to cultured cells without causing excessive hypertrophy or fibrosis. Previous studies demonstrate that 5–10% strain levels can provide effective mechanical cues toward robust development of sarcomeres that lead to enhanced contractility and intercellular communication through gap junction proteins like connexin-43 (Cx43).³⁵ Hence, we choose moderate strain levels of 7% to activate the mechano-transduction pathways. Figure 3B compares the real-time beating behavior of cardiomyocytes cultured on a flat circular PDMS diaphragm versus that on the AgNW-embedded nanogrooved circular PDMS diaphragm that is integrated with an EGaIn-based strain sensor. It is apparent

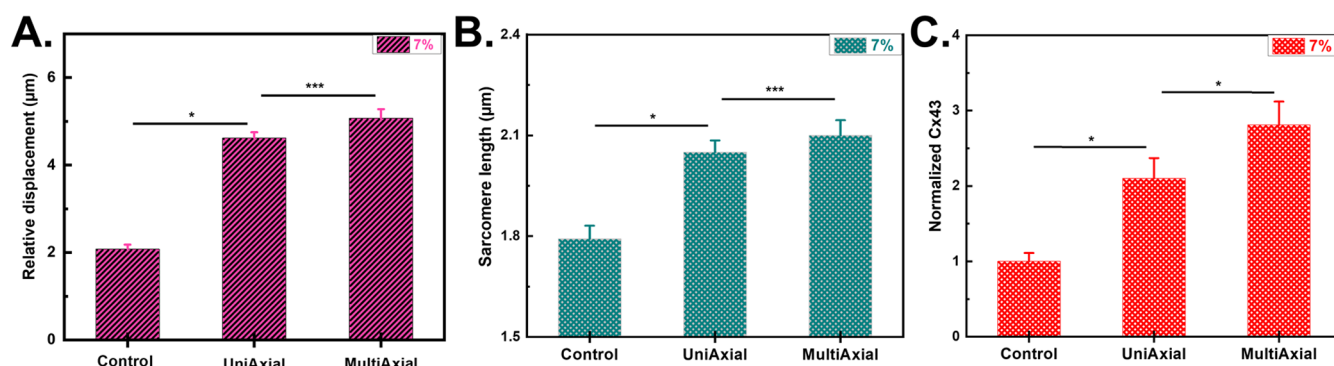


Figure 5. (A) Contractility of cardiomyocytes cultured under no stimulation on the flat PDMS surface, uniaxial stretching condition (AgNW-embedded nanogrooved rectangular diaphragm), and multiaxial stretching condition (AgNW-embedded nanogrooved circular diaphragm). (B) Quantitative analysis of sarcomere length of cardiomyocytes growing under different stretching conditions. (C) Change in connexin 43 expressions of cardiomyocytes growing under no stretching on the flat PDMS surface (control), uniaxial stretching, and multiaxial stretching conditions. (* $p < 0.05$ and *** $p < 0.005$, measured by one-way ANOVA test followed by Tukey's honest significant-difference test).

that cardiomyocytes cultured on the flat surface exhibit lower relative displacement and irregular beating behavior, indicative of functional immaturity. On the other hand, cardiomyocytes cultured on the AgNW-embedded nanogrooved circular PDMS diaphragm under mechanical stimulation exhibit regular and synchronized beating behavior, suggesting enhanced maturity. Furthermore, mechanical and topographical stimulation is reported to enhance the cytoskeletal organization of cultured cardiomyocytes.⁴¹ Indeed, more organized cardiomyocytes are observed when cultured on the AgNW-embedded nanogrooved circular diaphragm (see the inset). The synchronized beating behavior of cardiomyocytes (Supporting Information, Movie M1) is compared on various PDMS substrates (Figure 3C), including a flat circular diaphragm (control), AgNW-embedded circular diaphragm (AgNW), nanogrooved circular diaphragm (nG), nanogrooved circular diaphragm under mechanical stimulation (MS + nG), and the AgNW-embedded nanogrooved circular diaphragm under mechanical stimulation (MS + nG + AgNW). For the stimulated surfaces, mechanical stimulation was applied at a frequency of 1 Hz and at a strain level of 7%. The results indicate that cardiomyocytes cultured on the AgNW-embedded nanogrooved circular PDMS diaphragm could synchronize to the desired frequency under mechanical stimulation, whereas other platforms exhibited either irregular or asynchronous beating behavior (Figure 3C). This also influences the relative displacement profile of cardiomyocytes on these surfaces. The highest contractility is observed for cardiomyocytes cultured on the reported platform. Cardiomyocytes show increased sensitivity to their environment when cultured on an AgNW-embedded nanogrooved circular diaphragm, since the nanogrooves likely align the cardiomyocytes to affect their local microenvironment.⁴² Their highly synchronous behavior on the reported platform (Figure 3D) is attributed to the embedded AgNWs, which likely provide the needed conductivity to maintain cell-to-cell electrical signaling.

Enhancement of Protein Expression. The structural and functional characteristics of cultured cardiomyocytes were assessed based on their protein expression to assess their development toward a more specialized and functional state, like that found in adult heart tissue.⁴³ Immunocytochemistry (ICC) staining (details in the Materials and Methods section) was performed to image the protein expressions of cultured cardiomyocytes on various substrates. These include a flat

PDMS circular diaphragm (control), a nanogrooved circular PDMS diaphragm (nG), a nanogrooved circular PDMS diaphragm under mechanical stimulation (MS + nG), and a AgNW-embedded nanogrooved circular PDMS diaphragm under mechanical stimulation (MS + nG + AgNW). Comparing cardiomyocytes on the MS + nG + AgNW vs the control surface (Figure 4A), the mechanical stimulation (7% strain) impacts the extracellular matrix (ECM) via cell–cell interactions and the activation of stretch-activated ion channels. This stimulation significantly enhances the structural growth of cardiomyocytes on the MS + nG + AgNW surface vs. on the control. Notably, there were changes in protein expression, specifically, α -actinin and connexin 43 (Cx43). The altered expression of Cx43 indicates well-defined cell junctions and a higher level of protein expression in cardiomyocytes cultured on the reported platform vs on the flat PDMS surface. Figure 4B presents quantitative data on sarcomere length, highlighting that the cardiomyocytes cultured on the reported PDMS diaphragm (MS + nG + AgNW surface) exhibited the longest sarcomeres. Mechanical stimulation is correlated to this increase in the sarcomere length, likely by enhancing the sliding distance between actin and myosin filaments during contraction, thereby improving cardiomyocyte contractility. Comparison to other PDMS diaphragm surfaces suggests a correlation between increased sarcomere length and the greater average relative displacement of cells during contraction. Additionally, the nanogrooves aligned cardiomyocytes directionally and supported their structural development (see images of α -actinin stained and Cx43 stained cardiomyocytes in Supporting Information, Figure S6). Focal adhesion kinases play a crucial role in the cellular response to mechanical stimulation, potentially initiating a signaling cascade from the extracellular environment through focal adhesion complexes to the Z discs, a protein rich structure that anchors the actin rich filaments and maintains mechanical stability of cardiac muscles. This cascade likely facilitates mechanical interactions among cultured cardiomyocytes, contributing to enhanced sarcomere length.⁴⁴ Similarly, normalized Cx43 expression, crucial for gap junctions, followed a similar trend (Figure 4C). Elevated Cx43 expression levels suggest improved electrical signaling between cells, likely facilitated by enhanced electrical propagation across the AgNW-embedded nanogrooved surface and the development of more functional gap junctions under external mechanical stimulation.⁴⁵ ICC staining further demonstrates

enhanced electrical signaling between adjacent cardiomyocytes, synchronized contraction rates with the applied frequency, and coordinated beating. To further highlight the importance of synergistic stimulation with AgNW, nanogrooves, and controlled mechanical loading, additional control PDMS platforms without either nanogrooves or mechanical loading were investigated (Supporting Information, Figure S7). These show that AgNWs solely or in conjunction with mechanical stimulation but without nanogrooves failed to recreate similar cytoskeletal profiles within cultured cardiomyocytes. Hence, the synergistic combination of mechanical stimulation and AgNW-embedded nanogroove platforms is essential to promote regular cardiomyocyte beating, enhancing protein expression and structural growth.

Role of Multiaxial Stretching on Cardiomyocyte Cell Communication and Function. The native heart experiences multiaxial pneumatic pressure during its contraction and relaxation cycles, making multiaxial stretching a preferable *in vitro* model to uniaxial stretching to recapitulate multidirectional expansion and contraction for enhancing the structural integrity and function of cardiomyocytes.²⁹ Previous work focusing on uniaxial stretching to promote cardiomyocyte maturation has often failed to mimic the native cardiac microenvironment due to the static or repetitive nature of the stress that does not fully capture the dynamic and cyclic stresses present in native heart during beating,⁴⁶ leading us to investigate the effects of different stretching methods on cardiomyocyte structural enhancement. Using a flat PDMS surface as the control (Figure 5), we compare the structural and functional characteristics of the cultured cardiomyocytes obtained by applying uniaxial stretching on a rectangular nanogrooved PDMS diaphragm embedded with AgNWs to promote cell-to-cell interactions versus multiaxial strain applied using a circular PDMS diaphragm with embedded AgNWs, both under 7% strain. Our observations of cardiac contractility indicate that cardiomyocytes cultured on flat surfaces exhibit lower structural development compared with those subjected to either stretching method (Figure 5A). Protein expression analyses further supported these findings. Multiaxial strain showed a small but significant increase in cardiomyocyte contractile behavior compared with uniaxial strain, correlating with sarcomere length (Figure 5B) and improvements in beating behavior. Interestingly, cardiomyocytes under multiaxial stretching presented more significant enhancements in Cx43 protein expression compared to those under uniaxial stretching (Figure 5C). The possible explanation is that the multiaxial strain profile in the circular diaphragm likely maintained the integrity of the embedded AgNW mesh from all directions, unlike the possibility of disconnection under uniaxial stretching. Multiaxial stretching also likely ensures uniform stress distribution, promoting balanced cellular remodeling, cytoskeletal alignment, and well-organized sarcomere formation, which are critical for efficient cardiomyocyte function. Additionally, it likely fosters isotropic organization of the extracellular matrix, enhancing cellular interactions and mechanotransduction pathways that are crucial for growth, survival, and stress response of cardiomyocytes.⁴⁷ This balanced mechanical environment can reduce the risk of pathological remodeling associated with uniaxial stress, thereby supporting healthier and more functional cardiomyocytes. Hence, we infer that mechanical stimulation with the circular PDMS diaphragm to create multiaxial stretching is essential for

enhancing cardiomyocyte cell-to-cell communication and function.

CONCLUSIONS AND OUTLOOK

To advance the *in vitro* recapitulation of functional cardiomyocytes, we present a novel nanogrooved array platform embedded with silver nanowires (AgNWs) for biomimetic cell culture. Central to our innovation is a two-layer thin PDMS diaphragm design that electrically isolates the liquid metal strain sensor in the bottom layer, which is used to control the mechanical stimulation to cardiomyocytes from conductive portions of the top layer, which is optimized for the proportion of embedded AgNWs to support cardiomyocyte culture. The platform facilitates cardiomyocyte alignment, maturation, and functional synchronization through synergistic effects of surface cues for cell alignment, mechanical stimulation, and improved intercellular communication. Our findings highlight that cardiomyocytes cultured on this platform exhibit significant improvements in contraction force, sarcomere length, and connexin-43 (Cx43) expression, all of which are crucial for efficient cardiac function. Along similar lines from prior work wherein spatial organization and conductive biomaterials were shown to significantly enhance cellular functionality through electrical signaling⁴⁸ for developing functional tissue constructs,⁴⁹ the current work highlights integration of AgNWs within the nanogrooves for cell alignment coupled to effective electrical communication between cells to promote synchronized beating and robust structural development. Furthermore, mechanical stimulation with the circular PDMS diaphragm to create multiaxial stretching was essential toward enhancing cardiomyocyte cell-to-cell communications and function, along the lines of prior work on the role of biomechanical forces in cellular development and functionality for replicating the dynamic environment of heart tissue.⁵⁰ Based on the image analysis of Figure 3A, we estimate the cardiomyocyte volume change under multiaxial stretching conditions in the reported platform under 7% strain levels to be ~13% (see Supporting Information), which is in the range of 10–15% volume change of the heart during the cardiac cycle.⁵¹ These results indicate the potential of the arrayed nanogroove platform for high-throughput cardiac drug development and toxicity screening, making it a valuable tool in precision medicine applications using patient-derived materials. While the integrated strain sensor presents the potential for direct measurement of cell contractility rather than through the immunostaining methods performed in the current study, the bulky nature of the diaphragm (~300 μm thickness) in the reported platform limits the strain ranges that can be obtained for direct real-time contractility measurements. Recent advances in liquid metal patterning coupled to utilization of ultrathin diaphragms integrated with liquid metal sensors⁵² for direct cardiac contractility measurement can potentially address this limitation. Integration of the reported platform with upscaled cardiac models generated by emerging biofabrication technologies is of great interest.⁵³ Integration of the reported sensors and actuators with stimuli responsive materials is another worthy direction.⁵⁴ The integration of microelectrode arrays into the reported platform, to allow for *in situ* measurement of electrical activity in cardiac cells, will allow the measurement of physiological cues to cells. This will provide valuable insights into how cardiac cells respond to drugs, ultimately improving the accuracy and reliability of the

drug toxicity studies. Additionally, integrating real-time monitoring systems and advanced imaging techniques can enhance the platform's capabilities for in-depth analysis of cellular responses. Expanding this technology to include other cell types and tissues could pave the way for creating comprehensive *in vitro* models that better mimic the human physiological environment. Such advancements will be instrumental in advancing our understanding of cardiac diseases and developing more effective therapeutic strategies.

MATERIALS AND METHODS

Fabrication of Arrayed AgNW-Embedded Nanogrooved Circular Diaphragms. As shown in Supporting Information, Figure S1, the fabrication of arrayed AgNW-embedded nanogroove patterned PDMS circular diaphragm involves three steps: creating the AgNW-embedded nanogroove PDMS layer, making the microchannel PDMS layer, and bonding for EGAIn injection. First, a nanogrooved PDMS mold is formed using a prepatterned silicon mold. A degassed 10:1 PDMS mixture is applied to the silicon mold and cured at 80 °C for 2 h. After being cooled, the PDMS mold with the nanogroove pattern is separated from the silicon mold. PVA solution (0.3 g/mL) was applied to a 4-in. silicon wafer. The PDMS mold was pressed onto the PVA to transfer the nanopatterns, and then, the PVA was cured at 120 °C overnight. Finally, the PDMS mold was carefully removed, leaving the nanogrooves in the PVA layer. Then, AgNWs were spin-coated on the PVA layer. After that, PDMS mixed with a curing agent (10:1 ratio) was degassed in a vacuum desiccator for 30 min. It was then spin-coated onto a PVA mold at 500 rpm for 20 s. The coated mold was baked at 80 °C for 2 h and cooled to room temperature. After the PVA mold was dissolved in distilled water, the AgNW-embedded nanogroove patterned PDMS layer was obtained. The microchannel patterned PDMS layer was fabricated using soft photolithography. HDMS was spin-coated on a silicon substrate for 40 s at 4000 rpm. SU-8 3005 was then spin-coated for 40 s at 4000 rpm, baked at 95 °C for 3 min, exposed to UV light, and baked again. The substrate was developed in SU-8 developer for 2 min and hard-baked at 150 °C for 1 h. PDMS, mixed with a curing agent (10:1 ratio) and degassed, was spin-coated at 500 rpm for 20 s and baked at 80 °C for 2 h. Since both the nanogrooved and microchannel layers were over 100 μm thick, there was a distinct separation between the embedded AgNWs and the integrated EGAIn sensor, ensuring no interference from the AgNWs with the sensor's performance. An oxygen (O_2) plasma treatment was employed to bond the nanogrooved PDMS layer to the microchannel PDMS layer. Both layers underwent a 30 s treatment in oxygen plasma equipment at 80 W. This treatment facilitated the chemical bonding of the layers. Four circular diaphragms were then created using a 2 mm thick PDMS supporting framework and drilled to form 4 8 mm central holes corresponding to the diaphragm's diameter. Two additional holes were made near each hole for the EGAIn injection. Another plasma treatment with a phosphorus oxygen (O_2) bonded the PDMS supporting structure to the diaphragm. Finally, EGAIn was injected into the PDMS microchannel at a flow rate of 0.01 mL/min. Finally, the whole device was chemically bonded to glass to create an air channel for applying mechanical stimulation.

Characterization and Optimization of Embedded AgNWs in Diaphragms. The characterization of embedded silver nanowires (AgNWs) within the nanogrooved PDMS diaphragm was conducted by field emission scanning electron microscopy to visualize the distribution of AgNWs for highlighting the exposed and embedded regions within the PDMS matrix (Supporting Information, Figure S3a). Additionally, SEM-EDS elemental mapping provided confirmation of the presence of AgNWs interwoven throughout the substrate (Supporting Information, Figure S3b,c). Electrical properties of the AgNW-embedded PDMS surface were validated by four point probe measurement of surface conductivity, which demonstrated a surface conductivity of 1.5 $\text{M}\Omega$, which is within the physiologically relevant range of 2–400 $\text{M}\Omega$ observed in native myocardium. Since silver can oxidize and cause cardiotoxicity in

cultured cells, we identified optimal AgNW proportions for supporting the cardiomyocyte culture, while promoting electrical cell-to-cell communication. For this purpose, AgNW concentrations of 0.1, 0.2, and 0.3 mg/mL were embedded in nanogrooved circular PDMS diaphragms. Cardiomyocytes were then cultured on these substrates to determine the optimal AgNW concentration (Supporting Information, Figure S2).

Nanogrooved Array Setup. The experimental setup utilized an arrayed AgNW-embedded nanogrooved PDMS diaphragm with integrated EGAIn strain sensor integrated for culturing and maturing cells, particularly cardiomyocytes, providing structural stimulation. A custom stimulator, made of a solenoid pump and a LabVIEW program, applied periodic mechanical stimulation to the cells, monitored by a source meter measuring EGAIn strain sensor resistance changes. A stage top incubator with 5% CO_2 and a hot water cylinder maintained optimal culturing conditions. An inverted microscope facilitated live cell imaging and video acquisition to analyze the cardiomyocyte contractility. Cells were cultured on the AgNW-embedded nanogrooved circular PDMS diaphragm within the incubator at 37 °C for experimental observation and analysis. A schematic illustration of the system can be found in Supporting Information, Figure S8.

Cell Culture on Nanogrooved Array Platform. The H9C2 (2-1) cell line, derived from the embryonic rat heart tissue, was utilized in this work (American Type Culture Collection or ATCC, # CRL-1446). The cells were maintained in DMEM and supplemented with 10% fetal bovine serum (FBS) for growth. The cells were then incubated at 37 °C in a humidified incubator with 5% CO_2 to maintain proper pH. When cells reached 70–80% confluence, they were detached using 0.05% trypsin–EDTA. After the confluence, the serum concentration was reduced to 1% FBS, and 1 μM retinoic acid was added. They were then preplated and treated with O_2 plasma to enhance adhesion, dissemination, and proliferation. The cells were then seeded at a density of 1200 cells/ mm^2 on a fibronectin-coated, AgNW-embedded nanogrooved PDMS diaphragm. The cell culture medium was changed every 48 h.

ICC Staining. Immunocytochemical staining was conducted by using specific antibodies. Cardiomyocytes were fixed in 3.7% formalin for 10 min, washed with PBS, and permeabilized with 0.1% Triton-X in PBS for 10 min. Antibodies were blocked with 3% bovine albumin serum for 30 min. Primary antibodies for α -actin (1:100, Sigma), vinculin (1:100, Abcam), and integrin $\beta 1$ (1:100, Sigma) were diluted in a 1% blocking solution and incubated for 2 h. Secondary antibodies (Alexa-Fluor 488 goat antimouse IgG and Alexa-Fluor 568 rabbit) were diluted in the same blocking solution and incubated for 2 h. DAPI was used for nuclear staining for 20 min at 37 °C. Fluorescence imaging was performed using a confocal microscope.

Measurement of Contractility from Live Cell Imaging. Real-time images and videos of cardiac cell contractions were captured by using an inverted microscope. These recordings were analyzed with custom motion-tracking software. Initially, the videos were edited to the desired format with brightness and contrast normalized. The videos were then segmented into individual frames, and regions of interest were defined. Specifically, the edges of each cell were identified to determine their length in the relaxed state. During contraction, changes in the cell's length were measured using the software. A minimum of 10 cells from a single well were tracked, and their relative contraction displacements were measured. The average values of these displacements were utilized in this study.

Statistical Analysis. All statistical analyses were performed using the Origin Pro 2019 software. Each data set was generated from 5 samples and presented as mean values with the standard error of the mean (mean \pm SEM). Significance was calculated by utilizing the one-way ANOVA with Tukey's post hoc test, with $p \leq 0.05$ considered as significant and $p \leq 0.005$ considered as very significant.

■ ASSOCIATED CONTENT

SI Supporting Information

The Supporting Information is available free of charge at <https://pubs.acs.org/doi/10.1021/acsbiomaterials.4c01298>.

Fabrication process of arrayed AgNW-embedded nano-grooved circular PDMS diaphragm, optimization of AgNW concentration and embedded AgNW characterization, proof of a high throughput system, long-term stability of EGaln-based integrated sensor, orientation and protein expression of cultured cardiomyocytes on different surfaces, protein expression of cultured cardiomyocytes on AgNW-coated flat surfaces, and entire experimental setup (PDF)

Synchronized beating behavior of cardiomyocytes (MOV)

■ AUTHOR INFORMATION

Corresponding Author

Nathan S. Swami – Electrical and Computer Engineering, University of Virginia, Charlottesville, Virginia 22904, United States; Chemistry, University of Virginia, Charlottesville, Virginia 22904, United States; orcid.org/0000-0002-0492-1160; Email: nswami@virginia.edu

Authors

Abdullah-Bin Siddique – Electrical and Computer Engineering, University of Virginia, Charlottesville, Virginia 22904, United States

Keith A. Williams – Electrical and Computer Engineering, University of Virginia, Charlottesville, Virginia 22904, United States

Complete contact information is available at:

<https://pubs.acs.org/doi/10.1021/acsbiomaterials.4c01298>

Author Contributions

Abdullah-Bin Siddique: Conceptualization, Methodology, Validation, Investigation, Data curation, Formal analysis, Writing original Draft. **Keith A. Williams:** Supervision, Resources. **Nathan S. Swami:** Project administration, Supervision, Conceptualization, Resources, Funding acquisition.

Funding

This work was supported by the NCI Cancer Center grant P30 CA44579, U54 CA274499, AFOSR grants FA9550-24-1-0057 & FA2386-21-1-4070, and University of Virginia's Strategic Investment Fund to the Center for Advanced Biomanufacturing.

Notes

The authors declare no competing financial interest.

■ REFERENCES

- (1) Vaduganathan, M.; Mensah, G. A.; Turco, J. V.; Fuster, V.; Roth, G. A. The global burden of cardiovascular diseases and risk: a compass for future health. *J. Am. Coll. Cardiol.* **2022**, *80* (25), 2361–2371.
- (2) Reilly, L.; Munawar, S.; Zhang, J.; Crone, W. C.; Eckhardt, L. L. Challenges and innovation: Disease modeling using human-induced pluripotent stem cell-derived cardiomyocytes. *Front. Cardiovasc. Med.* **2022**, *9*, 966094.
- (3) Van Poll, M. L.; Zhou, F.; Ramstedt, M.; Hu, L.; Huck, W. T. A self-assembly approach to chemical micropatterning of poly (dimethylsiloxane). *Angew. Chem., Int. Ed.* **2007**, *46* (35), 6634–6637.
- (4) Berthier, E.; Young, E. W.; Beebe, D. Engineers are from PDMS-land, Biologists are from Polystyrenia. *Lab Chip* **2012**, *12* (7), 1224–1237.
- (5) Merkel, T. C.; Bondar, V. I.; Nagai, K.; Freeman, B. D.; Pinnau, I. Gas sorption, diffusion, and permeation in poly (dimethylsiloxane). *J. Polym. Sci., Part B: Polym. Phys.* **2000**, *38* (3), 415–434.
- (6) Kuddannaya, S.; Bao, J.; Zhang, Y. Enhanced in vitro biocompatibility of chemically modified poly (dimethylsiloxane) surfaces for stable adhesion and long-term investigation of brain cerebral cortex cells. *ACS Appl. Mater. Interfaces* **2015**, *7* (45), 25529–25538.
- (7) Lee, S.; Shin, H. J.; Yoon, S. M.; Yi, D. K.; Choi, J. Y.; Paik, U. Refractive index engineering of transparent ZrO₂-polydimethylsiloxane nanocomposites. *J. Mater. Chem.* **2008**, *18* (15), 1751–1755.
- (8) Etezadi, F.; Le, M. N. T.; Shahsavari, H.; Alipour, A.; Moazzezy, N.; Samani, S.; Amanzadeh, A.; Pahlavan, S.; Bonakdar, S.; Shokrgozar, M. A.; et al. Optimization of a PDMS-based cell culture substrate for high-density human-induced pluripotent stem cell adhesion and long-term differentiation into cardiomyocytes under a xeno-free condition. *ACS Biomater. Sci. Eng.* **2022**, *8* (5), 2040–2052.
- (9) Siddique, A. B.; Shanmugasundaram, A.; Kim, J. Y.; Roshanzadeh, A.; Kim, E. S.; Lee, B. K.; Lee, D. W. The effect of topographical and mechanical stimulation on the structural and functional anisotropy of cardiomyocytes grown on a circular PDMS diaphragm. *Biosens. Bioelectron.* **2022**, *204*, 114017.
- (10) Raj M, K.; Chakraborty, S. PDMS microfluidics: A mini review. *J. Appl. Polym. Sci.* **2020**, *137* (27), 48958.
- (11) Chen, W.; Lam, R. H.; Fu, J. Photolithographic surface micromachining of polydimethylsiloxane (PDMS). *Lab Chip* **2012**, *12* (2), 391–395.
- (12) Weibel, D. B.; DiLuzio, W. R.; Whitesides, G. M. Micro-fabrication meets microbiology. *Nat. Rev. Microbiol.* **2007**, *5* (3), 209–218.
- (13) Mata, A.; Fleischman, A. J.; Roy, S. Characterization of polydimethylsiloxane (PDMS) properties for biomedical micro/nanosystems. *Biomed. Microdevices* **2005**, *7*, 281–293.
- (14) Onal, S.; Alkai, M. M.; Nock, V. A flexible microdevice for mechanical cell stimulation and compression in microfluidic settings. *Front. Phys.* **2021**, *9*, 654918.
- (15) Pavesi, A.; Adriani, G.; Rasponi, M.; Zervantonakis, I. K.; Fiore, G. B.; Kamm, R. D. Controlled electromechanical cell stimulation on-a-chip. *Sci. Rep.* **2015**, *5* (1), 11800.
- (16) Dou, W.; Malhi, M.; Zhao, Q.; Wang, L.; Huang, Z.; Law, J.; Liu, N.; Simmons, C. A.; Maynes, J. T.; Sun, Y. Microengineered platforms for characterizing the contractile function of in vitro cardiac models. *Microsyst. Nanoeng.* **2022**, *8* (1), 26.
- (17) Stiefbold, M.; Zhang, H.; Wan, L. Q. Engineered platforms for mimicking cardiac development and drug screening. *Cell. Mol. Life Sci.* **2024**, *81* (1), 197.
- (18) Oynbaatar, N. E.; Lee, D. H.; Patil, S. J.; Kim, E. S.; Lee, D. W. Biomechanical characterization of cardiomyocyte using PDMS pillar with microgrooves. *Sensors* **2016**, *16* (8), 1258.
- (19) Tandon, N.; Marsano, A.; Maidhof, R.; Wan, L.; Park, H.; Vunjak-Novakovic, G. Optimization of electrical stimulation parameters for cardiac tissue engineering. *J. Regen. Med. Tissue Eng.* **2011**, *5* (6), e115–e125.
- (20) Sathaye, A.; Bursac, N.; Sheehy, S.; Tung, L. Electrical pacing counteracts intrinsic shortening of action potential duration of neonatal rat ventricular cells in culture. *J. Mol. Cell. Cardiol.* **2006**, *41* (4), 633–641.
- (21) Tandon, N.; Cannizzaro, C.; Chao, P. H. G.; Maidhof, R.; Marsano, A.; Au, H. T. H.; Radisic, M.; Vunjak-Novakovic, G. Electrical stimulation systems for cardiac tissue engineering. *Nat. Protoc.* **2009**, *4* (2), 155–173.
- (22) Shachar, M.; Benishti, N.; Cohen, S. Effects of mechanical stimulation induced by compression and medium perfusion on cardiac tissue engineering. *Biotechnol. Prog.* **2012**, *28* (6), 1551–1559.
- (23) Nunes, S. S.; Miklas, J. W.; Liu, J.; Aschar-Sobbi, R.; Xiao, Y.; Zhang, B.; Jiang, J.; Massé, S.; Gagliardi, M.; Hsieh, A.; et al. Biowire:

a platform for maturation of human pluripotent stem cell–derived cardiomyocytes. *Nat. Methods* **2013**, *10* (8), 781–787.

(24) Zhang, T.; Wan, L. Q.; Xiong, Z.; Marsano, A.; Maidhof, R.; Park, M.; Yan, Y.; Vunjak-Novakovic, G. Channelled scaffolds for engineering myocardium with mechanical stimulation. *J. Regen. Med. Tissue Eng.* **2012**, *6* (9), 748–756.

(25) Pavesi, A.; Adriani, G.; Rasponi, M.; Zervantonakis, I. K.; Fiore, G. B.; Kamm, R. D. Controlled electromechanical cell stimulation on-a-chip. *Sci. Rep.* **2015**, *5* (1), 11800.

(26) Nitsan, I.; Drori, S.; Lewis, Y. E.; Cohen, S.; Tzllil, S. Mechanical communication in cardiac cell synchronized beating. *Nat. Phys.* **2016**, *12* (5), 472–477.

(27) Sidorov, V. Y.; Samson, P. C.; Sidorova, T. N.; Davidson, J. M.; Lim, C. C.; Wikswo, J. P. I-Wire Heart-on-a-Chip I: Three-dimensional cardiac tissue constructs for physiology and pharmacology. *Acta Biomater.* **2017**, *48*, 68–78.

(28) Tan, W.; Scott, D.; Belchenko, D.; Qi, H. J.; Xiao, L. Development and evaluation of microdevices for studying anisotropic biaxial cyclic stretch on cells. *Biomed. Microdevices* **2008**, *10*, 869–882.

(29) Gopalan, S. M.; Flaim, C.; Bhatia, S. N.; Hoshijima, M.; Knoell, R.; Chien, K. R.; Omens, J. H.; McCulloch, A. D. Anisotropic stretch-induced hypertrophy in neonatal ventricular myocytes micropatterned on deformable elastomers. *Biotechnol. Bioeng.* **2003**, *81* (5), 578–587.

(30) Bird, S. D.; Doevendans, P. A.; Van Rooijen, M. A.; Brutel De La Riviere, A.; Hassink, R. J.; Passier, R.; Mummery, C. L. The human adult cardiomyocyte phenotype. *Cardiovasc. Res.* **2003**, *58* (2), 423–434.

(31) Papadacci, C.; Finel, V.; Provost, J.; Villemain, O.; Bruneval, P.; Gennisson, J. L.; Tanter, M.; Fink, M.; Pernot, M. Imaging the dynamics of cardiac fiber orientation in vivo using 3D Ultrasound Backscatter Tensor Imaging. *Sci. Rep.* **2017**, *7* (1), 830.

(32) Su, Y. H.; Chiang, P. C.; Cheng, L. J.; Lee, C. H.; Swami, N. S.; Chou, C. F. High aspect ratio nanoimprinted grooves of poly (lactico-glycolic acid) control the length and direction of retraction fibers during fibroblast cell division. *Biointerphases* **2015**, *10* (4), 041008.

(33) Dou, W.; Wang, L.; Malhi, M.; Liu, H.; Zhao, Q.; Plakhotnik, J.; Xu, Z.; Huang, Z.; Simmons, C. A.; Maynes, J. T.; et al. A microdevice platform for characterizing the effect of mechanical strain magnitudes on the maturation of iPSC-Cardiomyocytes. *Biosens. Bioelectron.* **2021**, *175*, 112875.

(34) Kim, J.; Shanmugasundaram, A.; Lee, C. B.; Kim, J. R.; Park, J. J.; Kim, E. S.; Lee, B. K.; Lee, D. W. Enhanced cardiomyocyte structural and functional anisotropy through synergetic combination of topographical, conductive, and mechanical stimulation. *Lab Chip* **2023**, *23* (20), 4540–4551.

(35) Jeong, Y. J.; Kim, D. S.; Kim, J. Y.; Oyunbaatar, N. E.; Shanmugasundaram, A.; Kim, E. S.; Lee, D. W. On-stage bioreactor platform integrated with nano-patterned and gold-coated PDMS diaphragm for live cell stimulation and imaging. *Mater. Sci. Eng., C* **2021**, *118*, 111355.

(36) Visser, T. D.; Oud, J. L.; Brakenhoff, G. J. Refractive index and axial distance measurements in 3-D microscopy. *Optik* **1992**, *90* (1), 17–19.

(37) Tani, H.; Tohyama, S. Human engineered heart tissue models for disease modeling and drug discovery. *Front. Cell Dev. Biol.* **2022**, *10*, 855763.

(38) Gintant, G.; Sager, P. T.; Stockbridge, N. Evolution of strategies to improve preclinical cardiac safety testing. *Nat. Rev. Drug Discovery* **2016**, *15* (7), 457–471.

(39) Smith, A. S.; Macadangdang, J.; Leung, W.; Laflamme, M. A.; Kim, D. H. Human iPSC-derived cardiomyocytes and tissue engineering strategies for disease modeling and drug screening. *Biotechnol. Adv.* **2017**, *35* (1), 77–94.

(40) Feiner, R.; Dvir, T. Tissue–electronics interfaces: from implantable devices to engineered tissues. *Nat. Rev. Mater.* **2017**, *3* (1), 17076.

(41) Stoppel, W. L.; Kaplan, D. L.; Black, L. D. Electrical and mechanical stimulation of cardiac cells and tissue constructs. *Adv. Drug Deliv. Rev.* **2016**, *96*, 135–155.

(42) Kim, H. N.; Jiao, A.; Hwang, N. S.; Kim, M. S.; Kang, D. H.; Kim, D. H.; Suh, K. Y. Nanotopography-guided tissue engineering and regenerative medicine. *Adv. Drug Deliv. Rev.* **2013**, *65* (4), 536–558.

(43) Funakoshi, S.; Fernandes, I.; Mastikhina, O.; Wilkinson, D.; Tran, T.; Dhahri, W.; Mazine, A.; Yang, D.; Burnett, B.; Lee, J.; et al. Generation of mature compact ventricular cardiomyocytes from human pluripotent stem cells. *Nat. Commun.* **2021**, *12* (1), 3155.

(44) Mansour, H.; De Tombe, P. P.; Samarel, A. M.; Russell, B. Restoration of resting sarcomere length after uniaxial static strain is regulated by protein kinase *Ce* and focal adhesion kinase. *Circ. Res.* **2004**, *94* (5), 642–649.

(45) French, K. M.; Maxwell, J. T.; Bhutani, S.; Ghosh-Choudhary, S.; Fierro, M. J.; Johnson, T. D.; Christman, K. L.; Taylor, W. R.; Davis, M. E. Fibronectin and cyclic strain improve cardiac progenitor cell regenerative potential in vitro. *Stem Cell. Int.* **2016**, *2016* (1), 8364382.

(46) Wanjare, M.; Huang, N. F. Regulation of the microenvironment for cardiac tissue engineering. *Regen. Med.* **2017**, *12* (2), 187–201.

(47) Sheehy, S. P.; Grosberg, A.; Parker, K. K. The contribution of cellular mechanotransduction to cardiomyocyte form and function. *Biomech. Model. Mechanobiol.* **2012**, *11*, 1227–1239.

(48) Dong, R.; Ma, P. X.; Guo, B. Conductive biomaterials for muscle tissue engineering. *Biomaterials* **2020**, *229*, 119584.

(49) Morsink, M.; Severino, P.; Luna-Ceron, E.; Hussain, M. A.; Sobahi, N.; Shin, S. R. Effects of electrically conductive nanobiomaterials on regulating cardiomyocyte behavior for cardiac repair and regeneration. *Acta Biomater.* **2022**, *139*, 141–156.

(50) McCain, M. L.; Parker, K. K. Mechanotransduction: the role of mechanical stress, myocyte shape, and cytoskeletal architecture on cardiac function. *Eur. J. Physiol.* **2011**, *462*, 89–104.

(51) Eden, M.; Kilian, L.; Frank, D.; Frey, N. Cardiac Mechanoperception and Mechanotransduction: Mechanisms of Stretch Sensing in Cardiomyocytes and Implications for Cardiomyopathy. In *Cardiac Mechanobiology in Physiology and Disease*; Springer International Publishing: Cham, 2023; pp 1–35.

(52) Kong, M.; Vong, M. H.; Kwak, M.; Lim, I.; Lee, Y.; Lee, S. H.; You, I.; Awartani, O.; Kwon, J.; Shin, T. J.; et al. Ambient printing of native oxides for ultrathin transparent flexible circuit boards. *Science* **2024**, *385* (6710), 731–737.

(53) Okhovatian, S.; Khosravi, R.; Wang, E. Y.; Zhao, Y.; Radisic, M. Biofabrication strategies for cardiac tissue engineering. *Curr. Opin. Biotechnol.* **2024**, *88*, 103166.

(54) Mehrotra, S.; Dey, S.; Sachdeva, K.; Mohanty, S.; Mandal, B. Recent advances in tailoring stimuli responsive hybrid scaffolds for cardiac tissue engineering and allied applications. *J. Mater. Chem. B* **2023**, *11*, 10297–10331.